

# Toward faster degradation for natural fiber reinforced poly(lactic acid) biocomposites by enhancing the hydrolysis-induced surface erosion

Lan Xie · Huan Xu · Ze-Pu Wang · Xu-Juan Li ·  
Jing-Bin Chen · Zi-Jing Zhang · Hua-Mo Yin ·  
Gan-Ji Zhong · Jun Lei · Zhong-Ming Li

Received: 20 October 2013 / Accepted: 2 January 2014 / Published online: 5 February 2014  
© Springer Science+Business Media Dordrecht 2014

**Abstract** The poor and uncontrollable biodegradability of poly(lactic acid) (PLA)-based materials is one of the fundamental limitations for widening their applications. To regulate the degradation of PLA/ramie fiber biocomposites, the hydrophilicity of the composites was modified to attract more water attack by introducing water-soluble poly(ethylene glycol) (PEG). Analyses by characterization of sample size, weight loss and microstructure offered intensive information on the degradation

behavior of PLA biocomposites. It was revealed that PEG indeed significantly enhanced the surface erosion process and thus facilitated the degradation rate. The biocomposite bar containing 15 wt% PEG completed degradation within 50 days, while only ~50 wt% mass lost for the control biocomposite sample without PEG. Morphological observation confirmed that PEG accelerated the penetration of outside water from the surface to the center driven by the diffusion-in process, which subsequently boosted the hydrolytic action of the PLA backbone ester groups. Our results indicated that the PEG induced water penetration governed the overall degradation kinetics. As a strong response to the degradation, the stiffness of the biocomposite bars suffered from drastic decrease while  $T_g$  varied in a climbing trend within the early stage. Microscopic examination of degradation solution formed during hydrolytic degradation of the PLA biocomposites suggested oligomers or lactic acid monomers were released to the solutions. It was of great interest to observe PEG dissolved in the alkaline solution speeded the ramie fibers breaking down to tiny fragments and cellulose macromolecules which further regenerated into cellulose aggregates in various fantastic appearances like coral-like leaves and pine needles. Our success in regulating the degradation of PLA biocomposites also provides an instructive approach for other PLA based materials.

**Electronic supplementary material** The online version of this article (doi:10.1007/s10965-014-0357-z) contains supplementary material, which is available to authorized users.

L. Xie · H. Xu · Z.-P. Wang · X.-J. Li · J.-B. Chen · Z.-J. Zhang ·  
H.-M. Yin · G.-J. Zhong (✉) · J. Lei (✉) · Z.-M. Li  
College of Polymer Science and Engineering, State Key Laboratory  
of Polymer Materials Engineering, Sichuan University,  
Chengdu 610065, Sichuan, People's Republic of China  
e-mail: ganji.zhong@scu.edu.cn  
e-mail: lejun@scu.edu.cn

L. Xie  
e-mail: lancysmile@163.com

H. Xu  
e-mail: lovexuhuan@163.com

Z.-P. Wang  
e-mail: 935909296@qq.com

X.-J. Li  
e-mail: lixujuan2000@163.com

J.-B. Chen  
e-mail: 2524923585@qq.com

Z.-J. Zhang  
e-mail: zijingzhang8@gmail.com

H.-M. Yin  
e-mail: scugfzyhm@163.com

Z.-M. Li  
e-mail: zmli@scu.edu.cn

**Keywords** Poly(lactic acid) · Natural fiber biocomposites ·  
Hydrolytic degradation · Surface erosion · Cellulose  
regeneration

## Introduction

With a green concept in recent years, synthetic biopolymers based on annually renewable resources hold the basis for the

twenty-first-century portfolio of eco-efficient, biodegradable and sustainable plastics [1–8]. Among the currently available synthetic biopolymers, poly(lactic acid) (PLA), derived from starch, sugars, etc., arguably represents the most promising category [9–13]. PLA is not only processable with most standard processing techniques and biocompatible [14], but also biodegradable in the natural environment compost and aqueous solution degradation [15–20]. As a versatile biopolymer with excellent mechanical performances, PLA has been commercially developed in a variety of applications in the biomedical and pharmaceutical fields [21–27], as well as increasingly used as a safe plastic for disposable consumer products such as packaging materials contacting daily foods without migrating any toxicity [28–31]. As a matter of fact, the most important quality specifications for PLA are satisfying biocompatibility and degradability [32]. In other words, a proper and controllable biodegradation rate against application environment and mechanical properties of PLA products is essential to match the morphology and properties during a given service life.

Unfortunately, PLA is not ideally suited to completely degrade in an acceptable short term, and PLA degrading organisms are sparsely distributed in soil environments [33, 34]. The unsatisfactory biodegradability has been proved by a wide range of PLA degradation research. For instance, after being buried in soil for up to 12 months, injection-molded pure PLA showed an extremely slow degradation and almost did not lose any weight [35]. Even when the specialized proteinase K was applied to create an enzymatic degradation for PLA films in a Tris–HCl buffer solution, the degradation rates were rather slow and the film surfaces appeared very smooth after enzymatic degradation for 24 h at 37 °C [36]. With an eye to minimizing the environmental impact of this plastic, it is urgent to develop biopolymers that can rapidly degrade from the action of naturally occurring circumstance. As a promising new trend, properly designed degradation can be utilized for the recycling, preparation, and modification of PLA-based materials [37].

It is clear that the kinetics of the penetration of outside water, which directly leads to the chemical cleavage of the ester linkage, plays a key role in regulating hydrolytic degradation of PLA [38]. Based on the current research, the hydrolytic degradation occurs in stages [39]. The molecular chains in the amorphous region are preferentially hydrolyzed due to the surface swelling induced by the diffusion of water into the material, then the hydrolytic cleavage of backbone ester bonds would lead to the scission of the main chains or side chains and lowering of molecular weight followed by intracellular uptake of oligomers and monomers. According to the features of hydrolytic degradation, several approaches are proposed to improve the degradation kinetics of PLA, such as copolymerization, manipulating material shape and surface structure, and

adding fillers and proteinase [40]. Modifying PLA films towards a bioactive surface through grafting with water-soluble polymers would enhance the polymer reactivity with water and accessibility of the ester groups to water and ultimately achieve faster degradation [41]. With the same principle, developing PLA block copolymers containing hydrophilic segments such as poly(ethylene glycol) (PEG) [42, 43], poly( $\beta$ -amino ester) and poly( $\epsilon$ -caprolactone) (PCL) [44], was proved to attract more hydrolysis attack and catalyze the degradation kinetics, as well as adding some hydrophilic fillers into PLA matrix [45]. Moreover, formation of a porous structure permitted the PLA bars to biodegrade and fragment more quickly due to the increased surface area contacting with water [35, 46]. Unfortunately, copolymerization means high production costs, while PLA biocomposites based on natural fillers usually slow degradation like pure PLA. Then, how can we achieve an industrially feasible modification approach for mass production of PLA based materials that can rapidly degrade? To deal with this problem, we set out to improve the intrinsic hydrophilicity of PLA to attract more hydrolytic attack, which can be achieved by introducing a hydrophilic phase during the common processing methods. This specific phase should be featured by favorable miscibility with PLA chains, short chains to enhance the molecular mobility of PLA, as well as desirable biocompatibility for green products. Naturally, PEG must be the compelling candidate. PEG with short chains is used here because it is capable of outstanding biocompatibility and miscible with amorphous PLA [3], which is particularly advantageous for the formation of a homogeneous modified system, and easy penetration of water.

In this work, we attempt to confirm the role of PEG in regulating the hydrolytic degradation behavior of PLA/natural fiber biocomposites, taking into account the attractive mechanical performances and full biodegradability featured in such a category of biocomposites [47, 48]. The results well admire our assumption. The creation of a strong hydrophilic phase where the water attack is facilitated can evidently advance the degradation of biocomposites. Moreover, the solution after degradation is carefully monitored. The direct observation of remaining species released to the solution reveals PEG simultaneously boosts the dissolution of ramie fibers into fantastic regenerated structures of cellulose molecules. The strategy proposed in this work, taking advantage of boosting the hydrophilicity of PLA matrix, will help shape a convenient approach to design biocomposites performing desirable mechanical performances and fast degradation that can satisfy the compostable plastic requirements as being disposed in the natural environment, as well as a wide range of other PLA based materials. It launches another fascinating task to be further explored.

## Experimental

### Materials

The PLA used in this work was commercial product from Nature Works Co. Ltd., USA (4032D, 96 % L-LA and 4 % D-LA). PEG (trade name Carbowax) with a nominal weight-average molecular weight of 3350 g/mol was purchased from Dow Chemical Co. Ltd., USA. Ramie fibers were kindly supplied by Yuzhu Plant Fiber Industrial, Sichuan, China, and were used as received. And digital photos of ramie fibers are shown in Fig. S1 of the Supporting Information.

### Sample preparation

To avoid hydrolysis, PLA, ramie fiber and PEG were sufficiently dried under vacuum overnight before extrusion or injection molding, and the preset drying temperatures for these materials were 100, 80 and 45 °C, respectively. A corotating twin screw extruder with a ratio of screw length to its diameter (L/D) of 40 was used to compound PLA, PEG and ramie fiber. Barrel temperatures in seven zones were held at 40, 80, 150, 180, 180, 180 and 170 °C from feed section to metering section, respectively. And the screw speed was constantly set at 150 rpm. PLA and PEG mixtures were fed into the feed section, and the PEG contents were set at 0, 5, 10 and 15 wt% based on the weight of PLA matrix. Meanwhile, the threadlike ramie fibers were fed into another port located in barrel of section 3 after the melting of PLA and PEG, the fiber content in biocomposites was fixed at 20 wt% based on the weight of PLA/PEG blends by controlling the feeding speed of PLA/PEG blends and ramie fibers.

The extruded compounds after drying were injection molded into standard dog-bone test samples utilizing a conventional injection molding machine (Nissin, Japan), and the barrel temperature profiles were set at 160, 180, 185 and 180 °C, respectively, while the injection pressure was held at 80 MPa. For the sake of brevity, the resultant injection-molded biocomposites with different PEG loadings will be referred to through this paper as PEG0, PEG5, PEG10 and PEG15 where the numbers indicate weight ratios of PEG to PLA matrix. For example, PEG0 represents the PLA biocomposites containing only 20 wt% ramie fiber, while PEG15 stands for the modified biocomposites containing 15 wt% PEG and 20 wt% ramie fiber.

### Hydrolytic degradation

The long-term hydrolysis degradation was performed by immersing the samples under alkaline hydrolytic conditions for up to 100 days, the alkaline solutions were prepared by dissolving 0.1 mol sodium hydroxide (NaOH) in 1 L distilled

water. The four types of PLA biocomposites samples immersed in four separate 1.5 L containers with 1 L alkaline solution were stored in a humidified and thermo-stable incubator at 37 °C. At each specific incubation time, weight of the composite materials, exterior and internal morphology, and the aqueous phase were measured.

### Differential scanning calorimeter (DSC)

A DSC 204 Phoenix (Netzsch Company, Germany) was carried out to probe the influence of PEG on the thermal behaviors of PLA biocomposites, majorly including glass transition temperature ( $T_g$ ) and crystallinity ( $\chi_c$ ). Specimens of the PLA biocomposites (around 5–6 mg), obtained from the intermediate region of the injection molded bars, were heated from 30 to 180 °C at a heating rate of 5 °C/min. The crystallinity can be calculated by subtracting the enthalpy of cold crystallization and pre-melt crystallization from the enthalpy of melting by using the Equation 1 presented below.

$$\chi_c = \frac{\Delta H_m - \Delta H_{cc} - \Delta H_{pc}}{\Delta H_m^0} \times 100\% \quad (1)$$

where  $\Delta H_m$  is the enthalpy of melting for PLA,  $\Delta H_{cc}$  is the enthalpy of cold crystallization,  $\Delta H_{pc}$  is the enthalpy of pre-melt crystallization, and  $\Delta H_m^0$  is the enthalpy of melting for a 100 % crystalline PLA taken as 93.7 J/g.

### Microbeam Two-Dimensional Wide-Angle X-Ray Diffraction (2D-WAXD)

A scanning microbeam 2D-WAXD experiment was further performed to determine crystalline morphology of both ramie fibers and PLA matrix simultaneously. In order to obtain a discernable X-ray scattering intensity, a piece of slice with a thickness of 1 mm was carefully machined from the PLA biocomposites, as clearly diagrammed in our previous work for the sake of brevity [3]. For the biocomposites prior to the hydrolytic degradation, the same position of tensile bar where the DSC specimens were acquired, while the sample surfaces for the biocomposites after 5-day degradation were characterized with the aim of detecting the alteration of crystalline morphology during the degradation process. The 2D-WAXD measurements were conducted on the synchrotron light source under room temperature at the beamline BL15U1 of Shanghai Synchrotron Radiation Facility (SSRF, Shanghai, China). The distance from sample to detector was 167.5 mm, and the wavelength of the monochromated X-ray was 0.154 nm. Then the 2D-WAXD images were collected with an X-ray CCD detector (Model Mar165, 2048 pixels×2048 pixels of 80  $\mu\text{m}$ ×80  $\mu\text{m}$ ).

## Mass loss

Weight loss of the biocomposite materials was evaluated by weighing the remaining samples during the hydrolytic degradation for every 5 days. The percentage of weight remaining was calculated from the following expression:

$$\text{Weight Remaining}(\%) = W_d/W_i \times 100\%$$

where  $W_d$  and  $W_i$  stands for the dry weight and initial weight of the samples, respectively. The dry weight was obtained after drying the degraded biocomposites at 45 °C under vacuum for 4 h.

## Dynamic mechanical analysis (DMA)

DMA was conducted to obtain thermomechanical properties and more distinct insights into the evolution of material properties during the early 10 days of the long-term hydrolytic degradation. After 10-day degradation, standard samples could not be obtained to meet the testing requirements because the serious breakdown of some specific samples. The DMA measurements were carried on a DMA Q800 (TA Instruments, USA) in a multifrequency strain mode with a dual cantilever clamp (the ASTM standard D4065). And the apparatus was operated with a frequency of 1Hz, over a temperature range of 20-150 °C at a heating rate of 3 °C/min.

## Scanning electronic microscopy (SEM)

The degraded composite materials were taken out from the NaOH solutions and dried at 45 °C under vacuum for 4 h. To observe the internal morphology, a small block was cut from the sample first, then the block was placed in liquid nitrogen for 0.5 h, ultimately the block was cryogenically fractured. Moreover, the remaining species after degradation for 20 and 100 days were dried at 40 °C for 24 h on cover glasses conducted on a Linkam CSS450 hot stage. Prior to the SEM observation, the original degraded surfaces, internal fractured surfaces and the dried remaining species were sputter-coated with gold, and the accelerated voltage was held at 5 kV.

## Polarized optical microscopy (POM)

POM was performed to identify the remaining species in the aqueous phase after hydrolytic degradation. Specifically, the degradation solution was shaken to obtain a uniform dispersion, then the well-distributed solution was carefully dripped onto a clean glass. An Olympus BX51 polarizing optical microscopy (Olympus, Tokyo, Japan) equipped with a MicroPublisher 3.3 RTV CCD was applied to observe the remaining species after degradation.

## Results and discussion

### Effect of PEG on the Crystalline Morphology of PLA Biocomposites Prior to Degradation

The crystalline morphology is a vital factor influencing the mechanical performances (Figs. S2-S4) and degradation properties of PLA, which is profoundly determined by a combination of DSC measurements (Fig. 1) and 2D-WAXD analyses (Fig. 2). The DSC results suggest that the addition of PEG indeed acts as a crystallization accelerator, leading to the substantial increase in the crystallinity. Specifically, the crystallinity for PEG0 stays at the lowest level of 9.8 %, steadily rising to 19.5 %, 23.0 % and 34.8 % as the PEG content of the modified biocomposites is regulated at 5, 10 and 15 %. The improved crystallization kinetics stems from the enhanced molecular mobility of PLA in the presence of flexible PEG chains, which can be evidenced by the fact that the  $T_g$  transition moves to lower temperatures (Fig. 1). The 2D-WAXD patterns produce the same results with the DSC results, as depicted in Fig. 2. The diffraction arcs of ramie fibers demonstrate their ordered alignment along the flow direction, primarily resulting from the inherent flexibility of ramie fibers. Moreover, the diffraction intensity of PLA crystals is gradually increased as PEG is added. We recently demonstrated prevailing, strong transcrystalline layers of PLA were preferably developed at the surfaces of ramie fibers with the aid of PEG, indicating the desirable synergistic effects of ramie fibers and PEG on accelerating the crystallization kinetics of PLA [49]. In the present work, the synergistic effects are applied to the practical processing of PLA biocomposites, permitting the nice chance to modify the crystalline morphology for PLA with poor crystallization ability [12].

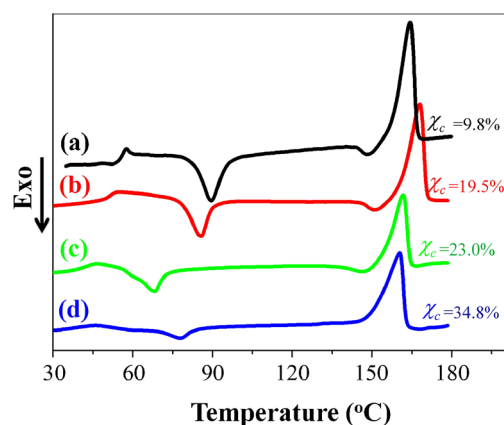


**Fig. 1** DSC traces recorded during the heating program, the crystallinity was calculated and the results were marked on the curves. **a** PEG0 biocomposite without PEG; **b-d** modified biocomposites PEG5, PEG10 and PEG15, containing 5, 10, and 15 wt% PEG, respectively

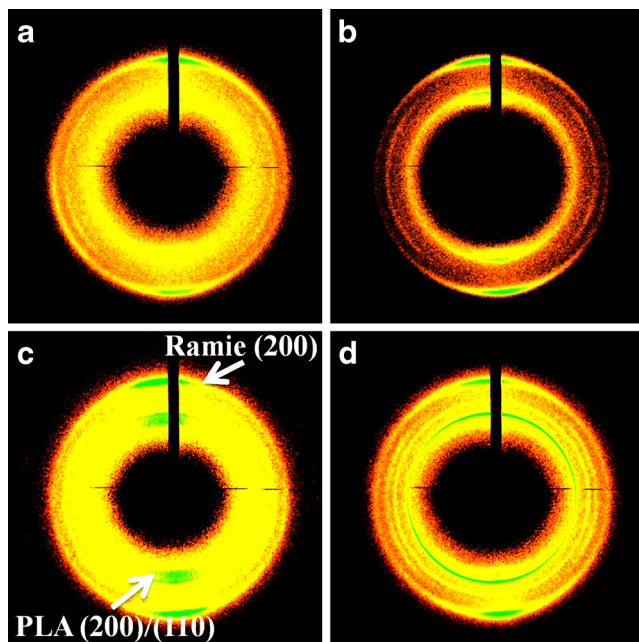
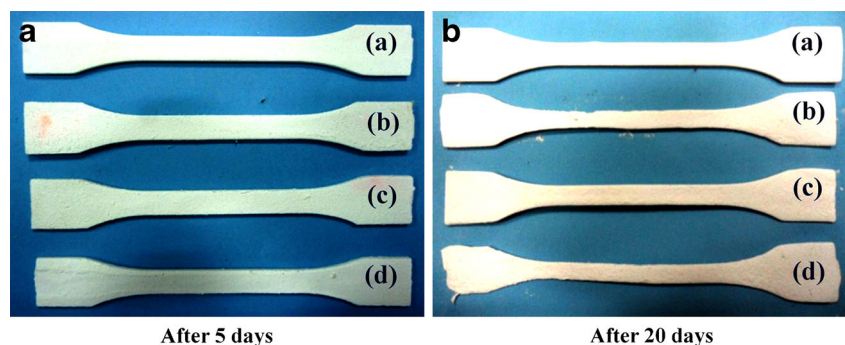


**Fig. 2** Representative 2D-WAXD patterns showing the morphology of ramie fibers and PLA, the corresponding diffraction reflections were marked in the image. **a** PEG0 biocomposite without PEG; **b-d** modified biocomposites PEG5, PEG10 and PEG15, containing 5, 10, and 15 wt% PEG, respectively

Evolution of visual aspect, mass and properties of PLA biocomposites during degradation

Measurements of visual aspect and mass variation provide direct evaluation of the degradation behavior of PLA biocomposites in the presence of PEG. Figure 3 shows the digital images of biocomposite bars after 5-day and 20-day degradation. In Fig. 3a, we can find the PEG0 sample still presents a smooth surface as the initial sample during the 20-day degradation, and the bulk length, width and thickness do not obviously vary either. In marked contrast, the modified biocomposites containing PEG suffer from obvious reduction in the bars' length, width and thickness, which is in proportion to the PEG content. Especially, after immersing for just 5 days, the surfaces of modified biocomposites turn to be rough where some fragments deviate from the PEG15 bar. Figure 3b

**Fig. 3** Digital photos of PLA/PEG/ramie fiber biocomposites after degradation in dilute alkaline solutions. **a** PEG0 biocomposite without PEG; **b-d** modified biocomposites PEG5, PEG10 and PEG15, containing 5, 10, and 15 wt% PEG, respectively



After 5 days

After 20 days

compares the visual aspects for the four PLA biocomposite bars degraded in the alkaline solutions for 20 days. Basically, the appearance of the PEG0 bar almost keeps unchanged. For the modified biocomposites, however, the thickness and width of all sample bars are further reduced apparently. Rapid hydrolytic degradation gives rise to the detachment of PLA matrix and ramie fibers, leaving obvious cavities in the surfaces of the biocomposite bars. The PEG15 one suffers from the most extensive breakage on every side of the bulk bar.

The quantitative analysis regarding the mass profiles of PLA biocomposites during hydrolytic degradation in alkaline solutions up to 100 days is plotted in Fig. 4. All samples rapidly lose their weight during the first 15 days. At the point of day 15, the remaining weight retains 70 % for PEG0, but declines to 61 %, 56 % and 38 % for PEG5, PEG10 and PEG15, respectively. Notice that the changes of the mass loss are larger than the content of the incorporated PEG. It is fairly concluded that the enhanced mass loss primarily stems from the accelerated degradation of PLA in the presence of PEG, which is probably assisted by the dissolution of PEG. After the fast degradation during the starting 15 days, the weight residue of PEG0 and PEG5 samples decreases at a low rate, generally displaying linear downtrends versus the degradation time and ultimately staying at 33 % and 18 % at the end of the 100-day degradation. In clear contrast, the weight residue of PEG10 and PEG15 maintains a fast decline throughout the entire degradation course. PEG10 degrades completely on day 70, while no remaining entities can be found for PEG15 after immersing in the alkaline solution for 50 days. It is noteworthy that the PEG15 sample loses over 90 % weight within 30 days, which desirably meets the standards for the definition of degradable materials [28].

The above results reveal that the PLA biocomposites without modification indeed present extremely slow degradation even in the alkaline solution. Shibata et al. acquired the similar results from composting degradation of pure PLA and PLA/abaca fiber biocomposite [50], in which no changes for the surface morphology and weight loss were observed for pure PLA after 180 days, while the composite sample only showed about 10 % weight loss. It has been well established that PLA degrades strictly through hydrolysis of its ester groups, followed by hydrolyzing into low molecular weight oligomers

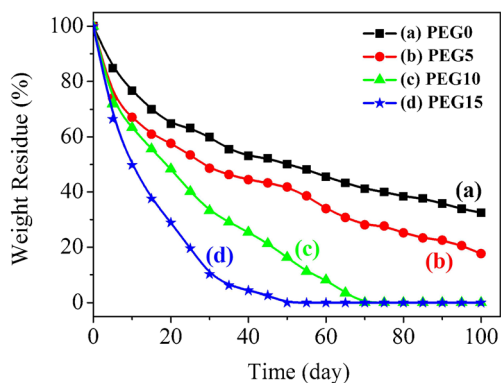


**Fig. 4** Weight residues of PLA/PEG/ramie fiber biocomposites as a function of degradation time during hydrolytic degradation for 100 days. **a** PEG0 biocomposite without PEG; **b–d** modified biocomposites PEG5, PEG10 and PEG15, containing 5, 10, and 15 wt% PEG, respectively

and finally mineralizing into  $\text{CO}_2$  and  $\text{H}_2\text{O}$  by the microorganisms existing in the environment [39, 51]. This can elucidate the reason for low degradation rate of PLA and its biocomposites, that is, the hydrolytic action of them is too weak [52]. Apparently, the scission of the main chains and the degradation rate profoundly depend on the penetration kinetics of water through the surface [44]. It can be exemplified by the faster degradation of PLA diblock or triblock copolymers containing superior-water-absorbing blocks such as PCL and PEG segments, compared to PLA homopolymers [42, 53, 54]. Of immense significance, too, is the observed fact that PEG15 presents the highest crystallinity but the optimal degradation rate. Although the crystallinity is substantially increased, herein the introduced PEG still enables PLA biocomposites degrade faster, there are two main reasons responsible for this: the rapid dissolution of PEG will guide neighboring water attaching onto the amorphous and crystallized PLA matrix [43], and the overall degradation rate can be further enhanced

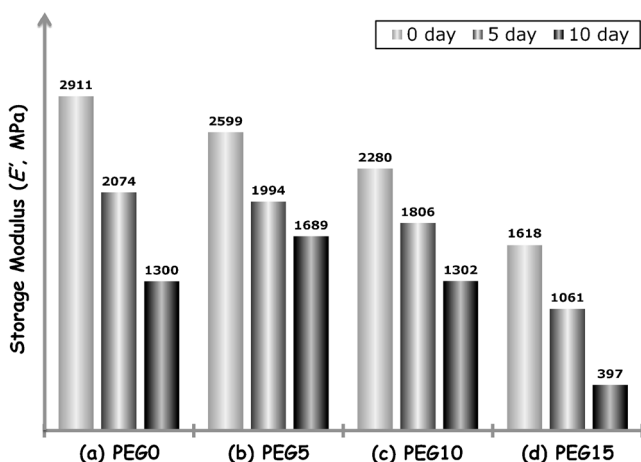


**Fig. 5** Dependence of storage modulus ( $E'$ ) at 25 °C on degradation time for the biocomposite materials containing various PEG contents. **a** PEG0 biocomposite without PEG; **b–d** modified biocomposites PEG5, PEG10 and PEG15, containing 5, 10, and 15 wt% PEG, respectively

by the release of more degraded species as a result of abundant interspace created via the prior dissolution of PEG chains [54].

DMA measurement was performed to track the evolution of dynamic mechanical performance of the PLA biocomposite samples after specific hydrolytic degradation periods, from which the storage modulus ( $E'$ ) and loss modulus ( $E''$ ) was obtained. Figure 5 compares  $E'$  at 25 °C for the biocomposites after 0, 5 and 10-day degradation. In the original state,  $E'$  drops from 2911 MPa for PEG0 down to 1618 MPa for PEG15. As the degradation proceeds,  $E'$  falls rapidly for all the biocomposites. For example, after 5-day degradation,  $E'$  decreases to around 2000 MPa for the PEG0 and PEG5 samples, and further declines to 1806 and 1061 MPa for PEG10 and PEG15 ones, respectively. After 10-day degradation,  $E'$  of these samples only reserves 1300, 1689, 1302 and 397 MPa, respectively. Similarly, Cheung's team observed the gradual deterioration of mechanical performances during the hydrolytic degradation process of PLA/silk biocomposites [55]. Several factors associated with the structural characters are responsible for the reduced stiffness along with the degradation process, including the formation of oligomers and monomers with extremely low molecular weight [56, 57], the preferential erosion of the interface between PLA and ramie fibers which significantly weakens the interfacial adhesion [50], and the deteriorated properties of ramie fibers caused by the simultaneous hydrolytic degradation in the alkaline solutions [58] (Fig. 7).

The degradation process would inevitably involve the profound variation of the high order structure. Physical parameters such as crystallinity, melting point and  $T_g$  are usually taken as reflective indicators related with the high order structure [44, 59–61]. Figure 6 describes the comparison of  $T_g$  collected from the  $E''$  curves of biocomposite samples at the time points of degrading for 0, 5 and 10 days. Immediately noticed from the  $T_g$  data, the original biocomposites have the widest  $T_g$  gap of all the

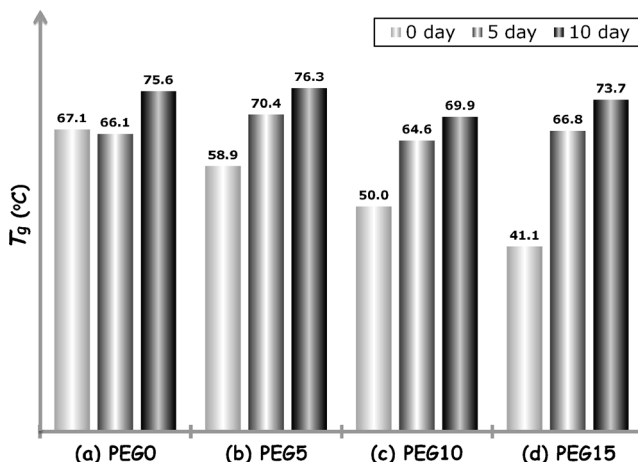
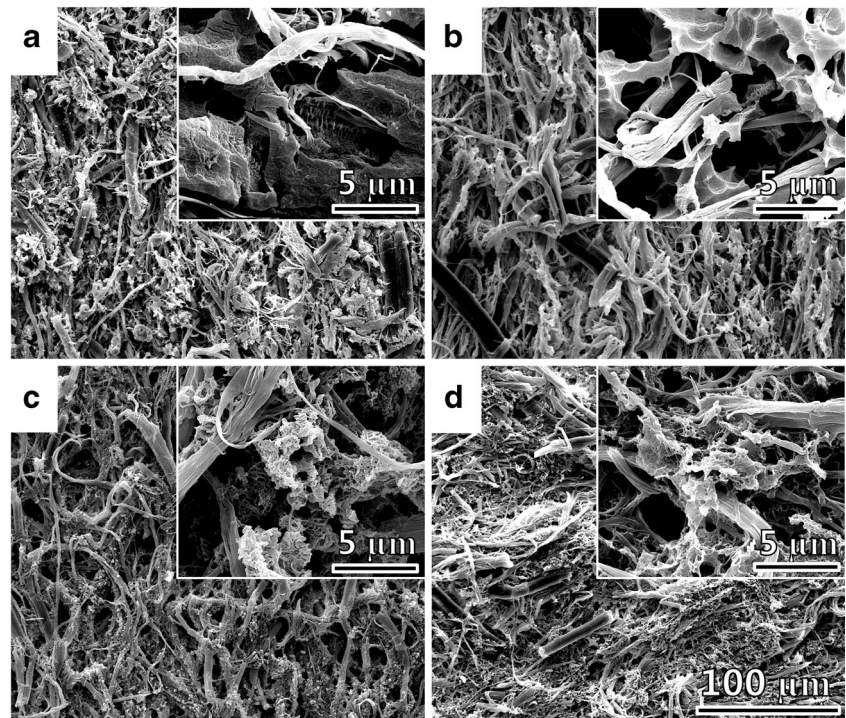


**Fig. 6** Dependence of glass transition temperature ( $T_g$ ) on degradation time for the four biocomposite materials. **a** PEG0 biocomposite without PEG; **b–d** modified biocomposites PEG5, PEG10 and PEG15, containing 5, 10, and 15 wt% PEG, respectively

**Fig. 7** SEM images of surface morphology of PLA/PEG/ramie fiber biocomposites after degradation for 5 days. **a** PEG0; **b** PEG5; **c** PEG10; **d** PEG15. The magnification factor is held constant for **a–d**, while the inset micrographs present the surface morphology in higher resolution



sample categories. PEG0 shows the highest  $T_g$  of 67.1 °C, then the  $T_g$  gradually falls to 58.9, 50.0 and 41.1 °C for the PEG5, PEG10 and PEG15 samples, respectively. The decreased  $T_g$  confirms the enhanced molecular mobility of PLA in the presence of PEG. Interestingly,  $T_g$  of all the biocomposites degraded for 5 days climbs up to approximately 67 °C and further rises to about 75 °C after 10 days. The significant increase of  $T_g$  expresses some conceivable structure changes. The depletion of PLA matrix causes the increase of relative ramie fiber content in the composites, and more ramie fibers are exposed to the solution. Meanwhile, the preferential erosion of amorphous PLA regions would result in the formation of rich crystalline regions that are more resistant to the hydrolysis erosion [60, 62, 63]. These two aspects, to a large extent, restrict the mobility of PLA chains. This result is well in-line with those previously reported for the growing  $T_g$  values as the degradation progressively develops [53, 57]. Briassoulis et al. investigated the degradation behavior of PLA films and fibers in soil under Mediterranean field conditions and laboratory simulations testing, and observed an increase of  $T_g$  values during the first 3 months [57]. On the contrary, other researchers detected downward trends in terms of assessing the  $T_g$  values of PLA [62–65]. As an example, Fukushima and his colleagues stated the degradation in compost lowered down the  $T_g$  values of PLA and PLA nanocomposite materials, and they supposed the plasticizing effect of oligomers and monomers released upon degradation would enhance the mobility of PLA chains [65]. In our case, the oligomers and monomers formed during the hydrolytic degradation of PLA are immediately dissolved in the solution. With this result the plasticizing effect is largely weakened compared to that of

composting degradation. Therefore,  $T_g$  variation is closely associated with the material characters and degradation environment. Up to date, a precise and comprehensive description of  $T_g$  transitions regarding the PLA degradation is still lacking, especially for a scientific consensus on understanding the underlying molecular mechanisms.

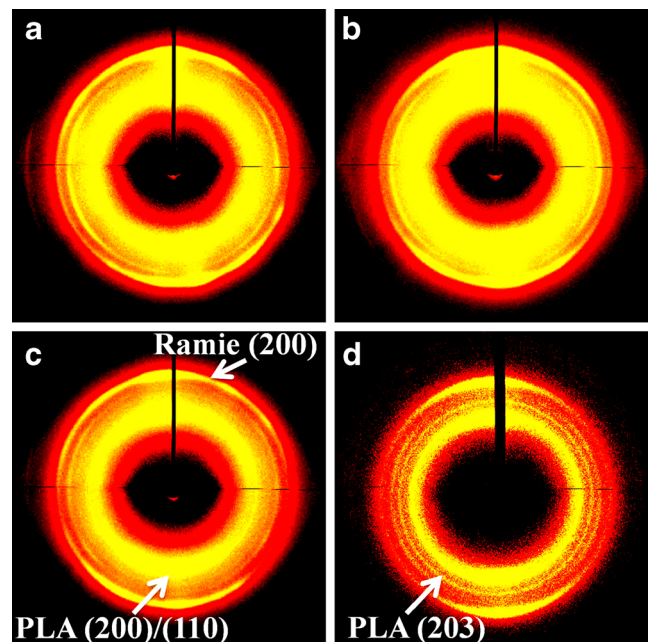
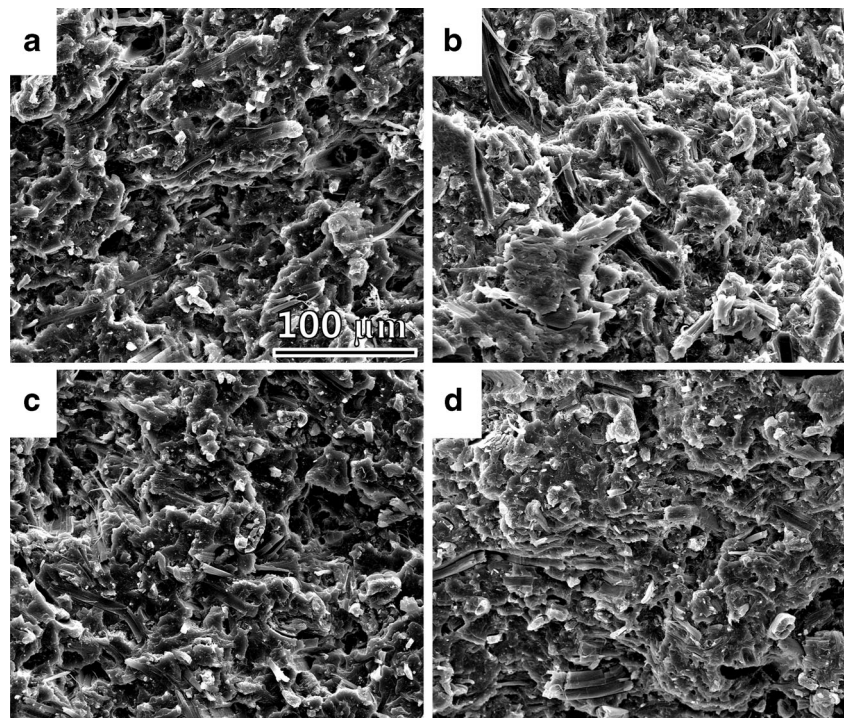


**Fig. 8** Typical 2D-WAXD patterns of crystalline morphology measured from the surfaces of PLA/PEG/ramie fiber biocomposites after degradation for 5 days. **a** PEG0; **b** PEG5; **c** PEG10; **d** PEG15. The corresponding diffraction reflections are marked in the images

**Fig. 9** SEM images of inner morphology of PLA/PEG/ramie fiber biocomposites after degradation for 5 days. **a** PEG0; **b** PEG5; **c** PEG10; **d** PEG15. The magnification factor is held constant for all images



#### Morphological observation of PLA biocomposites after degradation

It is well known that degradation proceeds along the weak paths from outside to inside of the polymer materials, which allows to suppose that the surface morphology observation can provide direct information on understanding the

degradation behaviors [35]. Figure 7 presents the micrographs for the surfaces of the PLA biocomposite samples incubated in alkaline solutions for 5 days. All the samples present rough surfaces covered with randomly dispersed ramie fibers, showing a great quantity of hollows consisting of uncovered fibers without traces of continuous bulk matrix. Only tiny PLA fragments are adhered onto the ramie fibers as representatively

**Fig. 10** SEM images of surface morphology of PLA/ramie/PEG fiber biocomposites after degrading for 40 days. **a** PEG0; **b** PEG5; **c** PEG10; **d** PEG15. The magnification factor is held constant for all images

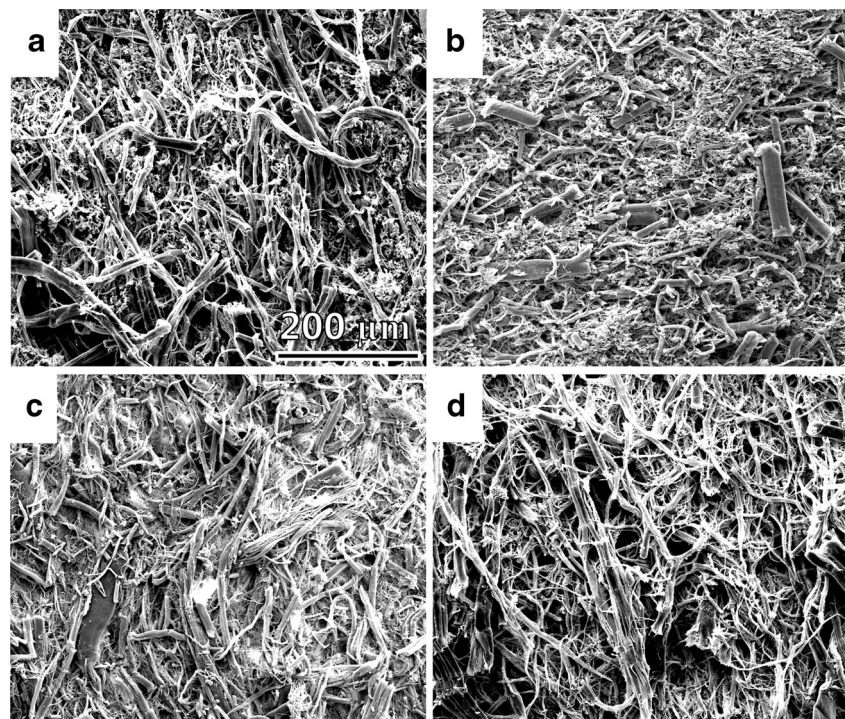
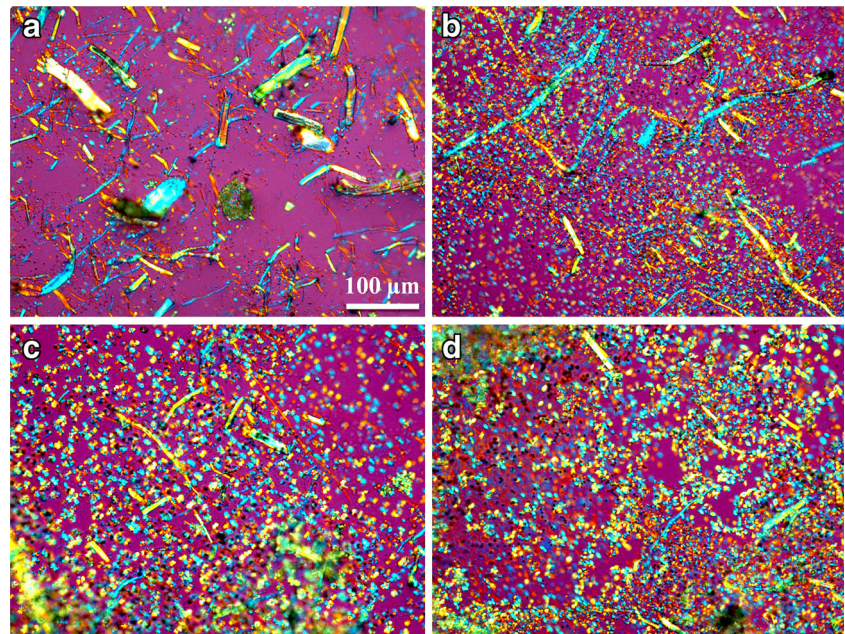




**Fig. 11** POM observations of remaining species in the aqueous phase after degradation for 10 days. The magnification factor is held constantly for all micrographs. **a** PEG0; **b** PEG5; **c** PEG10; **d** PEG15



shown in the inset micrographs. These tiny particles are probably crystalline PLA entities because the crystalline part of the PLA is more resistant to degradation than the amorphous part [39, 46]. The crystalline regions only undergo hydrolysis when the sample is being degraded for a longer time, which reasonably leads to the gradual increase of the apparent crystallinity along with the degradation time [40, 66]. It is evident that the fast degradation of amorphous regions in PEG10 and PEG15 resulted in the formation of crystalline structures throughout the bulk of the biocomposites after just 5 days. This is also corroborated by their  $T_g$  results (cf. Fig. 6).

Taking advantage of the high spatial resolution of microbeam 2D-WAXD, the surface crystalline morphology for the biocomposites after degradation for 5 days was further detected (Fig. 8). Two important features of 2D-WAXD patterns that distinguish the degraded samples from those of the original biocomposites (Fig. 2) are clearly observed: 1) The diffraction intensity of the lattice plane (200) of cellulose I in microfibril crystals of ramie fibers becomes stronger. It is presumably due to more ramie fibers are exposed to the degradation environment after the gradual depletion of the PLA matrix, as observed in SEM micrographs (Figs. 7). 2) Apparently the diffraction reflections of PLA crystals achieves much higher intensity compared to those presented in the original biocomposites (Fig. 2). Such an increase of diffraction intensity, in effect, is indicative of the presence of more crystals on the surfaces after the degradation process which primarily attacks the amorphous phase. Thus it confirms the hypothesis that the tiny particles wrapping the ramie fibers are principally the crystalline entities as observed in Fig. 7.

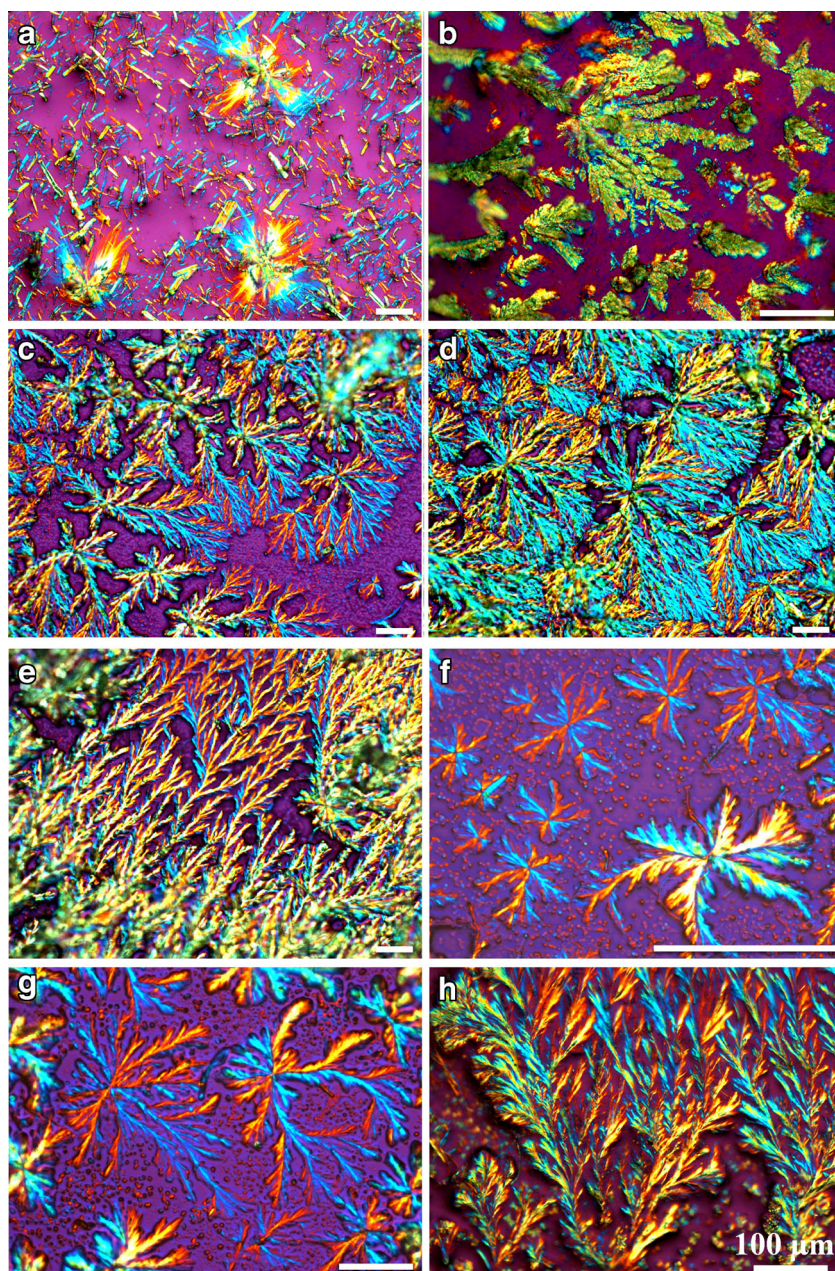
Figure 9 compares the internal morphology of the PLA biocomposite bars after 5-day degradation. It can be observed that the continuous PLA bulk matrix is well retained and the ramie fibers are buried in the intact matrix. Apart from this, the addition of PEG does not alter the inner morphology, and no obvious difference is observed among PEG0 and modified biocomposites. The injection-molded biocomposite samples are relatively thick (ca. 4 mm), giving rise to the fact that the permeation of water into the interior of the biocomposite bars is fairly slow. This supports the theory that a hydrolytic process occurring at the material surface plays the key factor to the faster degradation of the solid PLA [67]. The similar results were obtained by Cheung and his coworkers who observed the fractured surfaces of silk reinforced PLA biocomposites at some specific time points [55]. Moreover, Tomita et al. [33] and Shogren et al. [35] observed the degradation gradually spread throughout the PLA sample, and assumed the degradation of PLA occurred on the surface of the solid sample and not inside. On the basis of those sufficient evidence, it is anticipated that the penetrating water creates a negative gradient from the surface to the bar center, which is expected to drive the diffusion-in process for the water molecules [63].

The surfaces of the biocomposite bars after 40-day degradation are shown in Fig. 10. What is immediately noticeable from Fig. 10a–b is that the PEG0 and PEG5 bars after degradation for 5 days (see Fig. 7) and 40 days present similar surface morphology. Ramie fibers randomly distribute on the surfaces without any trace of continuous bulk PLA matrix, and some tiny fragments adhered to fibers spread throughout the overall surfaces. Interestingly, Fig. 10c–d suggests only smooth ramie fibers which wrap around each other are presented on the surfaces of PEG10 and PEG15, and no PLA

fragments stay in the vicinity of ramie fibers. The digestion of tiny fragments is probably caused by the profound scission of PLA chain backbone at the later period near the completion of degradation for the PEG10 and PEG15 samples containing higher contents of PEG. The increase in PEG content facilitates the hydrolysis kinetics of PLA ester bonds and the overall degradation rate. It is reasonably concluded that PEG10 and PEG15 are more susceptible to surface erosion and their mass loss falls more quickly compared to PEG0 and PEG5, which is clearly demonstrated in Figs. 10 and 4, respectively. It in turn confirms PLA degrades through hydrolysis, and the hydrolytic degradation of PLA depends primarily on the kinetics of the chemical cleavage of the ester linkage. The hydrolysis of ester

bonds can only occur during the direct contact with water, and the diffusion of water into the solid bar plays a significant role in deciding the degradation rate of PLA [68]. Recently, Albertsson's research group demonstrated the degradation process and resulting degradation product patterns were significantly altered by modifying PLA surface through grafting acrylic acid, facilitating the rapid formation of water-soluble degradation products [41]. In our case, introducing water-soluble PEG into the PLA matrix can profoundly improve the water diffusion into the bar, thereby largely enhancing the PLA reactivity with water and accessibility of the ester groups to water and catalyst, i.e., NaOH molecules, and finally the degradation is notably accelerated.

**Fig. 12** POM observations of remaining species in the aqueous phase after degradation for 100 days. **a–b** PEG0; **c–d** PEG5; **e–f** PEG10; **g–h** PEG15. All the scale bars present 100  $\mu\text{m}$



Direct observation of remaining species in the aqueous phase

The PLA hydrolysis starts with the diffusion of water into the matrix and thus a great number of degradation experiments are based on aqueous solutions [36, 43]. However, no information is available on the characterization of remaining species which are released into the aqueous phase during degradation, despite this is of major importance for medical applications as bioresorbable materials. We here attempt to directly observe the morphology of the remaining species in the degradation solution for the first time. Figure 11 presents the POM micrographs of remaining species after immersing the biocomposite bars for 10 days. Randomly dispersed ramie fibers that suffer varying degrees of degradation are immediately observed in Fig. 11, and the degradation degree appears in proportion to PEG content. Figure 11 also suggests that no massive PLA particles can be observed in all degradation solutions. Specifically, Fig. 11a shows numerous massive ramie fibers accompanied by a few point-like ramie aggregates appear in PEG0. As the PEG content increases, the massive ramie fibers gradually turn into tiny point-like ramie aggregates in terms of the declining length and diameter as depicted in Fig. 11b–d. Prevailing point-like aggregates except for few thread ramie fibers densely distribute in the aqueous phase of PEG15. PEG in the modified biocomposites tends to rapidly dissolve in the NaOH solution, which offers a nice chance for boosting hydrolytic degradation of ramie fibers into tiny species and cellulose molecules under the combined effects of PEG and NaOH. It shares the same results with Yan and Gao's work, in which the PEG/NaOH aqueous solution system was developed to sufficiently dissolve

cellulose with a long period of stability [58]. The solution containing 1 wt% PEG and 9 wt% NaOH was revealed to be a direct cellulose solvent rather than a derivative aqueous solution system. The underlying mechanism is far from clarity. PEG molecules likely act as the hydrogen-bonding acceptor that prevents the re-association of hydroxyl groups of cellulose. Moreover, the missing of massive PLA particles clearly states that PLA deviated from the biocomposite bars is absolutely degraded into oligomers or lactic acid monomers soluble in the water. The hydrolytic degradation of PLA is a very complex process involving various diffusion–reaction phenomena such as water absorption, ester bond cleavage, diffusion and solubilization of soluble species [54].

The aqueous phase after immersing the biocomposite bars for 100 days is also taken for POM observation. Figure 12 shows no trace of massive PLA particles, however, ramie cellulose in the aggregative state derived from ramie fibers is clearly observed, instead of separate ramie fibers as presented in Fig. 11. The ramie cellulose aggregates into various morphologies, such as radial cross-shaped spheres (Fig. 12a) and coral-like leaves (Fig. 12b) for PEG0, fish scale-shaped aggregates closely distributed for PEG5 (Fig. 12c–d), pine needles regularly aligned along one direction (Fig. 12e) and hexapetalous stars with a diameter of tens micrometer for PEG10 (Fig. 12f) for PEG10, and huge star-shaped brachiaria ramosa (Fig. 12g) and gorgeous peacock tails spread up straight (Fig. 12h) for PEG15. The fantastic and multiple morphologies of the cellulose aggregates are attributed to the hydrolytic dissolution of ramie fibers into cellulose macromolecules followed by the regeneration of the dissolved cellulose macromolecules [58]. The structure of the aggregated cellulose in the degradation solutions of the modified biocomposites containing PEG is

**Fig. 13** POM observations of remaining species in the aqueous and dried phase after degradation for 100 days. **a** degradation solution for pure PLA; **b** degradation solution for ramie fibers; **c** dried remaining species for PEG10 after the water is absolutely volatilized; **d** dried remaining species for PEG10 heated up to 190 °C to melt PLA, PEG and NaOH on a Linkam CSS450 hot stage. The scale bar present 100  $\mu\text{m}$  for all images

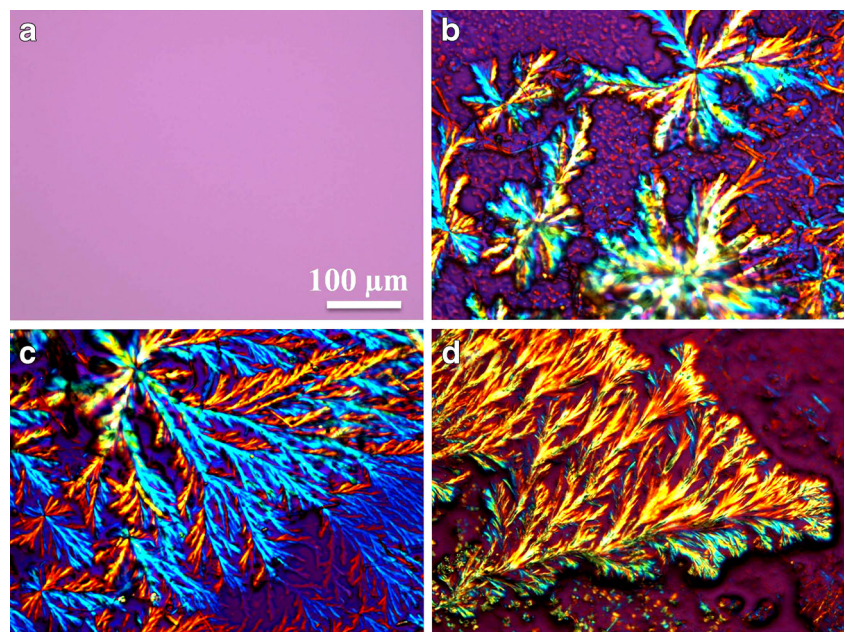
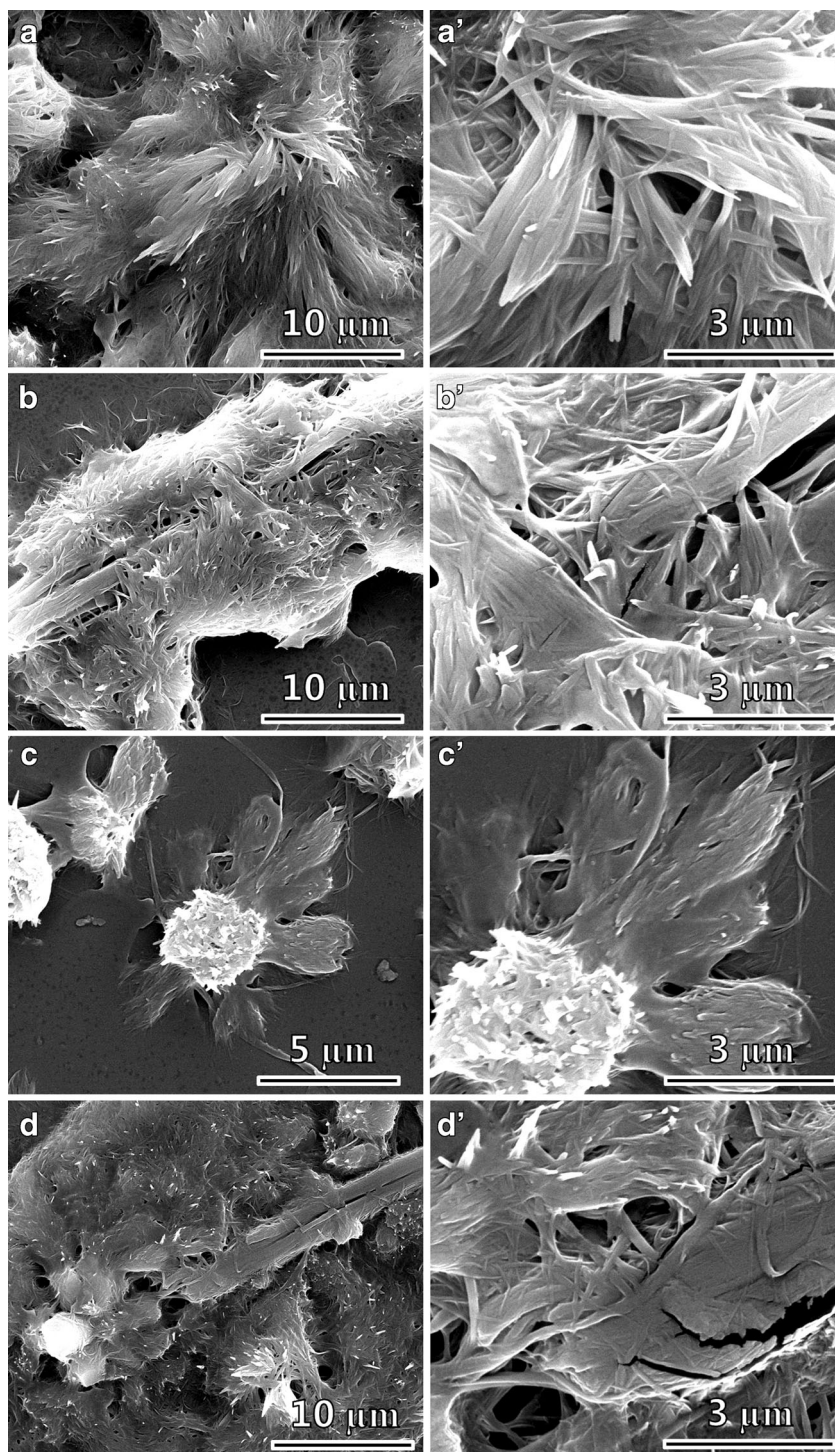


**Fig. 14** SEM observations of remaining species in the dried phase after degradation for 20 days. **a** PEG0; **b** PEG5; **c** PEG10; **d** PEG15. Prior to the SEM observation, the water is absolutely volatilized at 40 °C for 24 h on a Linkam CSS450 hot stage. (**a'**)–(**d'**) represent the SEM images in higher magnification for (**a**)–(**d**), respectively



evidently loose than that of the binary biocomposites without PEG. The PEG molecules in the aqueous solution systems own powerful capability to accept the hydrogen-bonding from the end groups of ramie cellulose, preventing the re-association of hydroxyl groups of cellulose to form compactly aggregates like the case of PEG0. As a result, the dissolved cellulose molecules regenerate into various patterns within a certainly separated space for the modified biocomposites. As for the type of these

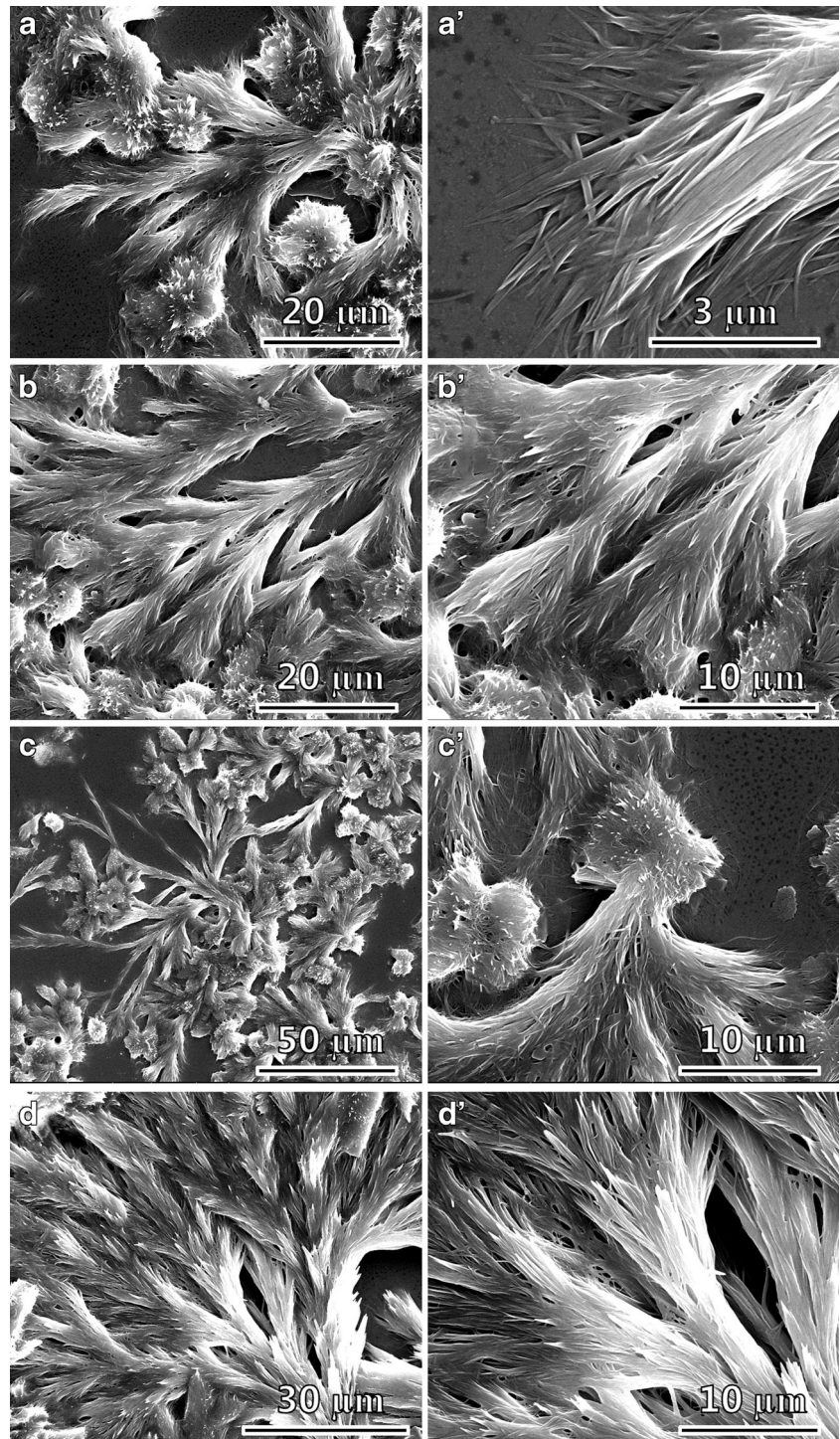
cellulose crystals, we reasonably anticipate it is mainly a source of microfibril crystals of ramie fibers in the form of cellulose I, based on the observed diffraction patterns of the lattice plane (200) for the ramie cellulose. In other words, the degradation process are not expected to alter the crystal form of cellulose crystals.

To offer direct evidence for the formation of cellulose aggregates are observed in the degradation solution as

shown in Fig. 12, we further design a series of POM observation for confirming the source of the remaining species (Fig. 13). Figure 13a delineates the degradation solution in the aqueous phase for pure PLA. No visible particles or patterns are traced, demonstrating the degradation species of PLA are basically soluble, such as PLA oligomers and lactic acid monomers. It also indicates that the aggregated patterns do not derive from the degradation products of PLA.

In clear contrast, Fig. 13b confirms the formation of cellulose aggregates in the alkaline solution stems from the degradation of ramie fibers, while the influence of PEG and PLA is both removed. Moreover, the cellulose aggregates in the appearance of stars and peacock tails are still observed for the degraded PEG10 in the dried state (Fig. 13c) and after the sample is heated up to 190 °C to melt PLA, PEG and NaOH (Fig. 13d). Therefore, it is fairly concluded that the observed

**Fig. 15** SEM observations of remaining species in the dried phase after degradation for 100 days. **a** PEG0; **b** PEG5; **c** PEG10; **d** PEG15. Prior to the SEM observation, the water is absolutely volatilized at 40 °C for 24 h on a Linkam CSS450 hot stage. (**a'**)–(**d'**) represent the SEM images in higher magnification for (**a**)–(**d**), respectively



aggregates exactly originate from the regeneration of cellulose macromolecules, rather than the PLA oligomers, lactic acid monomers, water phase, PEG chains or NaOH crystals. We unearth these amazing morphologies of aggregated cellulose molecules can be formed during dissolving ramie fibers. It arouses our great interests, and exploration towards understanding the underlying mechanisms will be further carried out.

More evidences verifying the resource of the aggregated structure are offered by the SEM observation of the remaining species after degradation (Figs. 14 and 15). After degradation for 20 days, Fig. 14 evidently reveals that cellulose sheets with a width of around several hundred nanometers and a length over 20  $\mu\text{m}$  derive from the disassembly of ramie fibers. In the manner of aggregation, these cellulose sheets orderly pack into flower-like superstructure. The tree branch-like cellulose aggregation is observed for the remaining species after degradation for 100 days (Fig. 15). These observations emphasize that the origination of flower- and branch-like structures, exactly, relies on the dissolution of ramie fibers into less ordered sheets and cellulose macromolecules.

## Conclusions

Biocomposites based on biodegradable PLA and renewable natural fibers offer great potential for achieving low-cost manufacturing of green, high-performance plastics. However, the slow degradation rate of PLA poses challenges to rapid dispose of the used commodities. Here, we demonstrate an approach—facilitating the hydrophilicity of PLA by introducing the water-soluble PEG—that allows for a faster hydrolytic degradation of PLA. Ramie fiber reinforced PLA biocomposites featuring varying PEG contents (from 0 to 15 wt%) and fixed 20 wt% ramie fibers were prepared and investigated for their hydrolytic degradation behavior in alkaline solutions. PEG chains miscible with amorphous PLA drastically enhanced the penetration of water from bar surface to the center, accelerating the PLA degradation into oligomers and lactic acid monomers through hydrolysis cleavage of PLA ester bonds. Weight loss measurements suggested the weight residue of the PEG0 sample decreased at the lowest rate, ultimately staying at 33 % at the end of the 100-day degradation. In clear contrast, PEG15 lost over 90 % weight after 30 days and completed the degradation within 50 days, which desirably meets the standards for the definition of degradable materials. On the other hand, PEG dissolved in water facilitated ramie fibers breaking down to tiny fragments and cellulose macromolecules, which further regenerated into various aggregated structures such as coral-like leaves and gorgeous peacock tails. Dynamic mechanical properties monitored by DMA demonstrated stiffness of biocomposite bars suffered distinct deterioration within the hydrolytic

degradation, while  $T_g$  gradually climbed up to higher values due to the preferential erosion of amorphous PLA. Except for the great success in regulating the degradation PLA/natural fiber biocomposites, the instructive approach proposed here is very likely to find widespread applications for other PLA based materials, a fascinating task to be further explored.

**Acknowledgments** The authors gratefully thank the financial support from the National Natural Science Foundation of China (Grants 51120135002, 51121001, 51203104, and 50925311).

## References

- Xu H, Teng C, Mao Z, Yu M (2012) *J Polym Res* 19:9960
- Wang ZY, Li XW, Li JN, Li GM, Tao JQ (2009) *J Polym Res* 16:255
- Xu H, Zhong GJ, Fu Q, Lei J, Jiang W, Hsiao BS, Li ZM (2012) *ACS Appl Mater Interfaces* 4:6774
- Lee LT, Wu MC, Lee MH (2013) *J Polym Res* 20:282
- Wang ZY, Luo YF, Ye RR, Song XM (2011) *J Polym Res* 18:499
- Zhu MQ, Xiang L, Yang K, Shen LJ, Long F, Fan JB, Yi HQ, Xiang J, Aldred M (2012) *J Polym Res* 19:9808
- Kaczmarek H, Nowicki M, Vuković-Kwiatkowska I, Nowakowska S (2013) *J Polym Res* 20:91
- Bao D, Liao X, He T, Yang Q, Li G (2013) *J Polym Res* 20:290
- Kulinski Z, Piorkowska E, Gadzinowska K, Stasiak M (2006) *Biomacromolecules* 7:2128
- Amirian M, Nabipour Chakoli A, Sui J, Cai W (2012) *J Polym Res* 19:9777
- Hu X, Xu JZ, Zhong GJ, Luo XL, Li ZM (2011) *J Polym Res* 18:675
- Kaavessina M, Ali I, Elleithy R, Al-Zahrani SM (2012) *J Polym Res* 19:9818
- Luo SH, Wang QF, Xiong JF, Wang ZY (2012) *J Polym Res* 19:9962
- Hamad K, Kaseem M, Deri F (2011) *J Polym Res* 18:1799
- Bagheri M, Bigdeli E (2013) *J Polym Res* 20:84
- Lai SM, Lan YC (2013) *J Polym Res* 20:140
- Radjabian M, Kish MH, Mohammadi N (2012) *J Polym Res* 19:9870
- Shih YF, Huang CC (2011) *J Polym Res* 18:2335
- Wang L, Zhang Z, Chen H, Zhang S, Xiong C (2010) *J Polym Res* 17:77
- Wang L, Chen H, Zhang L, Chen D, Pang X, Xiong C (2011) *J Polym Res* 18:329
- Wang T, Jiang M, Wu Y (2010) *J Polym Res* 17:335
- Suwantong O, Pankongadisak P, Deachathai S, Supaphol P (2012) *J Polym Res* 19:9896
- Liu CC, Chang KY, Wang YJ (2010) *J Polym Res* 17:459
- Bagheri M, Motirasoul F (2013) *J Polym Res* 20:59
- Khamlao W, Hongeng S, Sakdapipanich J, Nasongkla N (2012) *J Polym Res* 19:9834
- Chanlen T, Hongeng S, Nasongkla N (2012) *J Polym Res* 19:36
- Azizi M, Farahmandghavi F, Joghataei M, Zandi M, Imani M, Bakhtiari M, Dorkoosh F, Ghazizadeh F (2013) *J Polym Res* 20:110
- Dorgan JR, Braun B, Wegner JR, Knauss DM (2006) Poly(lactic acids): a brief review. In: Khemani KC, Scholz C (eds) *Degradable polymers and materials. Principles and practice* Ch. 7. American Chemical Society, Washington, D.C, p 102
- Chen HC, Tsai CH, Yang MC (2011) *J Polym Res* 18:319
- Yeh J, Tsou C, Li Y, Xiao H, Wu C, Chai W, Lai YC, Wang CK (2012) *J Polym Res* 19:9766
- Liao X, Nawaby A (2012) *J Polym Res* 19:9827
- Chakoli A, Sui J, Amirian M, Cai W (2011) *J Polym Res* 18:1249

33. Tomita K, Tsuji H, Nakajima T, Kikuchi Y, Ikarashi K, Ikeda N (2003) *Polym Degrad Stab* 81:167
34. Gallet G, Lempiäinen R, Karlsson S (2000) *Polym Degrad Stab* 71:147
35. Shogren RL, Doane WM, Garlotta D, Lawton JW, Willett JL (2003) *Polym Degrad Stab* 79:405
36. Kurokawa K, Yamashita K, Doi Y, Abe H (2008) *Biomacromolecules* 9:1071
37. Tsuji H (2010) Hydrolytic degradation. In: Auras R, Lim LT, Selke SEM, Tsuji H (eds) *Poly(lactic acid): synthesis, structures, properties, processing, and applications*, vol 10. Wiley, Hoboken, p 345
38. Metters AT, Bowman CN, Anseth KS (2000) *J Phys Chem B* 104:7043
39. Tokiwa Y, Calabia BP (2006) *Appl Microbiol Biot* 72:244
40. Gorrasi G, Pantani R (2013) *Polym Degrad Stab* 98:1006
41. Höglund A, Hakkarainen M, Edlund U, Albertsson AC (2010) *Langmuir* 26:378
42. Stefani M, Coudane J, Vert M (2006) *Polym Degrad Stab* 91:2554
43. Shah NM, Pool MD, Metters AT (2006) *Biomacromolecules* 7:3171
44. Cohn D, Hotovely Salomon A (2005) *Biomaterials* 26:2297
45. Pradhan R, Misra M, Erickson L, Mohanty A (2010) *Bioresource Technol* 101:8489
46. Odelius K, Höglund A, Kumar S, Hakkarainen M, Ghosh AK, Bhatnagar N, Albertsson AC (2011) *Biomacromolecules* 12:1250
47. Xu H, Liu CY, Chen C, Hsiao BS, Zhong GJ, Li ZM (2012) *Biopolymers* 97:825
48. Xu H, Xie L, Chen YH, Huang HD, Xu JZ, Zhong GJ, Hsiao BS, Li ZM (2013) *ACS Sustainable Chem Eng* 1:1619
49. Xu H, Xie L, Jiang X, Li XJ, Li Y, Zhang ZJ, Zhong GJ, Li ZM (2013) *J Phys Chem B*. doi:10.1021/jp409021q
50. Teramoto N, Urata K, Ozawa K, Shibata M (2004) *Polym Degrad Stab* 86:401
51. Jarerat A, Pranamuda H, Tokiwa Y (2002) *Macromol Biosci* 2:420
52. Ahn HK, Huda MS, Smith MC, Mulbry W, Schmidt WF, Reeves JB (2011) *Bioresource Technol* 102:4930
53. Li S, Anjard S, Rashkov I, Vert M (1998) *Polymer* 39:5421
54. Huang MH, Li S, Vert M (2004) *Polymer* 45:8675
55. Cheung HY, Lau KT, Pow YF, Zhao YQ, Hui D (2010) *Compos Part B* 41:223
56. Agatemor C, Shaver MP (2013) *Biomacromolecules* 14:699
57. Rudnik E, Briassoulis D (2011) *Ind Crop Prod* 33:648
58. Yan L, Gao Z (2008) *Cellulose* 15:789
59. Höglund A, Odelius K, Albertsson AC (2012) *ACS Appl Mater Interfaces* 4:2788
60. Ishii D, Ying TH, Mahara A, Murakami S, Yamaoka T, Lee W, Iwata T (2009) *Biomacromolecules* 10:237
61. Pantani R, Sorrentino A (2013) *Polym Degrad Stab* 98:1089
62. Hakkarainen M, Karlsson S, Albertsson AC (2000) *Polymer* 41:2331
63. Regnell Andersson S, Hakkarainen M, Inkinen S, Södergård A, Albertsson AC (2012) *Biomacromolecules* 13:1212
64. Li S, McCarthy S (1999) *Biomaterials* 20:35
65. Fukushima K, Giménez E, Cabedo L, Lagarón JM, Feijoo JL (2012) *Polym Degrad Stab* 97:1278
66. Luo YB, Wang XL, Wang YZ (2012) *Polym Degrad Stab* 97:721
67. Andersson SR, Hakkarainen M, Albertsson AC (2013) *Polymer* 54:4105
68. Janorkar AV, Metters AT, Hirt DE (2004) *Macromolecules* 37:9151